What We Learn From Boiling under Microgravity

J. Straub, M. Zell and B. Vogel

LATTUM
Laboratory for Applied Thermodynamics and
Technology under Microgravity
Technical University Munich, Germany

Abstract

Boiling is a very efficient mode of heat transfer and is therefore employed in most thermal energy conversion and transport systems as well as in component heating and cooling. Due to the great density difference between the liquid and vapor phase, it is generally assumed that the transport mechanism is strongly influenced by buoyancy forces. Therefore, gravity is seen as an important factor in all physical based or empirical correlations for pool boiling heat transfer. Only tests in a microgravity environment provide a means to study the real influence of gravity and to isolate gravity dependent from gravity independent factors.

During the last 10 years we were able to carry out boiling experiments at low gravity in ballistic rocket flights within the German TEXUS program and in parabolic flights with aircraft (KC 135) from NASA at Houston. Our findings were surprising that in nucleate boiling over a wide range of fluid states and heat fluxes, the heat transfer coefficient is hardly influenced by lower acceleration, which is in strong contradiction to the present picture of boiling, and the predictions of extrapolated equations. Thus, the boiling process can also be used for space applications as an effective heat transfer mechanism for thermal power generation, cooling devices and other heat exchangers.

At the present stage, however, the study of details of the boiling mechanism is much more significant. If gravity is not the primary force to determine boiling heat transfer, what other mechanisms are able to provide these high heat flux rates? The solution of this complex task is the common goal of the scientific cooperation with Japanese scientists, who support the research program by own experiments using drop shafts, parabolic flights, sounding rockets rockets and Get Away Special facilities. This report is concerned with a short summary of results obtained by the authors.

1. Introduction and Objectives

Since the first boiling curve obtained by Nukiyama (1934) /1/, many investigations on boiling and two-phase flow heat transfer have been performed in the past fifty years. Nevertheless, the interest in boiling heat transfer is growing continually, documented by the numerous publications that appear in journals and conference proceedings. Dhir /2/ quoted two reasons for this increasing interest in his keynote presentation at the 9th International Heat Transfer Conference, Jerusalem (1990):

1. „Boiling is a very efficient mode of heat transfer and as such is employed in component cooling and in various energy conversion systems. The quest for improvement in the performance of the equipment and the demand imposed by new high density energy systems continue to motivate studies on boiling heat transfer."
2. „Boiling is a extremely complex and illusive process, which continues to baffle and challenge inquisitive minds."

We continue with Dhir's comment:

> „Unfortunately, for a variety of reasons, fewer studies have focused on the physics of the boiling process than have been tailored to fit the needs of engineering endeavors. As a result, the literature has been flooded with correlations involving several adjustable parameters. These correlations can provide quick input to design performance and safety issues and hence are attractive on a short-term basis. However, the usefulness of the correlations diminishes very rapidly as parameters of interest start to fall outside the range of physical parameters, for which the correlations are developed. Also, correlations involving several empirical constants tend to cloud the physics. Thus, if we wish to reduce the repetition of experimental effort in response to changes in the physical parameters of interest in an engineering enterprise, it is important to place greater emphasis on fundamental understanding of this process. A persistent effort in this direction will go a long way in transforming studies of boiling heat transfer from an art to a science and would be attractive and exciting to new researchers."

We fully agree with this statement, and our experience in studying the effect of gravity as a variable parameter results in the same: "the usefulness of the correlations diminishes very rapidly" outside the range of earth gravity. This result may indicate that the physics of the boiling process is indeed not properly understood and is poorly represented in most correlations, if they are extrapolated to lower or higher acceleration values than earth gravity can provide.

The boiling process is very complex owing to the interaction of numerous factors and effects, as the interaction between the solid surface of the heater with the liquid and vapor, interaction between liquid and vapor itself, and the transport of liquid and vapor. Thus the microgravity environment offers the unique opportunity to study these interaction processes without, or at least with reduced buoyancy forces. Larger bubbles are generated so that optical observations can be employed to study the fundamentals of boiling.

2. Boiling technology

A heat transfer process between a solid surface, heated or cooled, and a fluid is generally described by Newton's law:

$$\dot{Q} = \alpha \cdot A \cdot (T_w - T_\infty) \tag{1}$$

Where $\dot{Q}$ is the transfered heat flux, α is called the heat transfer coefficient, A is the area involved in the heat transfer, T_w is the surface temperature of the solid wall, and T_∞ is the bulk fluid temperature in some distance from the wall. If a certain heat flux $\dot{Q}$ is transferred in technological processes, the area A and the temperature difference $(T_w - T_\infty)$ should be as small as possible; the first one for a smaller design of the heat exchanger and for the reduction of material and investment costs, and the second for higher efficiency of the thermal process. As a result, the heat transfer coefficient α should be as high as possible. Boiling heat transfer coefficients are some orders of magnitude higher than those in single phase flows. Therefore, the boiling process has a great technological significance.

The heat transfer coefficient in boiling is a complex function combining many different interacting parameters. These are: the heater geometry, heater material, surface structure and roughness, nucleate site density, dynamic wetting behavior, thermophysical properties of solid, liquid and vapor, the fluid state (saturated or subcooled), the vapor pressure and the heat flux. Moreover, many of these parameters are temperature dependent. Therefore, the usual manner to describe transport problems in fluid motion by solving the partial differential equations of the conservation laws can not be applied. Boiling heat transfer correlations are therefore based on optical observations and experimental data and can generally only be applied within the range of parameters, for which they are developed. For more general application in heat transfer, dimensionless parameters such as Nu-, Re-, Ra- and Fo-numbers were often formed to make the correlations independent from the applied scale. As a characteristic length scale in boiling, the Laplace coefficient L or the departure diameter D of the bubble, according to Fritz (1935, /3/), is used most frequently written with variable system acceleration:

$$D = C \cdot L\,(a/g)^{-1/2} = C \cdot \left(\frac{\sigma}{g(\rho_l - \rho_g)}\right)^{1/2} (a/g)^{-1/2} \tag{2}$$

where σ is the surface tension, ρ_l and ρ_g are the densities of the liquid (index l) and vapor (index g). C is a factor related to the wetting angle between the solid surface and the liquid, g the earth gravity and a the actual system acceleration. The departure diameter increases with a decreasing fraction a/g.

Thus it is evident that even in empirical correlations the actual acceleration is an important factor. Up to the present, no efforts have been made to verify experimentally how the influence of gravity can be correctly modelled in the boiling correlation. Therefore, as it will be shown later, it is not surprising that the existing correlations are quite contradictory in their representation of the influence of gravity.

3. The heat transfer modes in boiling

The various modes of heat transfer in boiling are demonstrated with the boiling curve or the so-called Nukiyama curve, Fig. 1. The most important modes are described shortly:

Fig. 1 Sketch of a boiling curve with the various modes of heat transfer

Convection, transient heat conduction

The first mode of heat transfer to a liquid from a heated surface with an increasing heat flux is at 1g-condition convection, A-B. The convection flow is due to a pressure difference either caused by buoyancy, called free convection, or by an imposed pressure difference along or across the surface, called forced convection. In microgravity, if forced convection is excluded, the first mode of heat transfer is transient conduction, A′- B′.

Nucleation

With increasing surface temperature, the liquid boundary layer will exceed saturation temperature and vapor bubbles appear on the heated surface, point B, B′. These bubbles are generated in cavities by heterogenous nucleation or by cavities containing a vapor embryo, called nucleate sites, and activated at a certain superheat of the liquid.

Nucleate boiling

By the inception of boiling, the wall superheat is reduced to C and C′, and single bubbles appear on the surface. With an increase of heat flux, more nucleate sites are activated and bubbles are generated with increasing frequencies. This mode of heat transfer is called nucleate boiling and is the most important one in the technological processes, C-D. In this region, the surface temperature increases only slowly for large changes in the heat flux. This can be expressed by a simple power law relationship:

$$\dot{q} \sim (\Delta T_{sat})^m \tag{3}$$

where $\dot{q} = \dot{Q}/A$ is the heat flux density, $\Delta T_{sat} = T_w - T_{sat}$ is the temperature difference between the surface temperature of the wall T_w and saturation temperature of the liquid T_{sat} corresponding to the saturation pressure. The exponent m depends on the fluid and nucleation properties and is found to be within 2.5 to 4.

Critical heat flux

If any attempt is made to increase the value of the heat flux above E, the surface temperature will suddenly jump from E to F, the next stable operating point in the film boiling region. In many practical cases, this large temperature jump is sufficient to cause dangerous situations, like the melting of the heater surface. Hence, the term "burn-out" or "boiling crisis" is frequently used to refer to this phenomenon. The heat flux in point E is called the "critical heat flux", CHF; and D-E is the region where hydrodynamic instabilities occur before CHF.

Film boiling

The next stable mode of heat transfer on the curve is called "film boiling", F-G. At large temperature differences a continuous vapor film blankets the heater surface. The major resistance in the heat transfer is confined to this vapor film. This region is the most tractable one for theoretical studies, due to the fact that there is no contact between the liquid and the solid. The heat transfer coefficients of laminar or turbulent films for various geometries can be derived in direct analogy to the relations of filmwise condensation, based on Nusselt's film theory for condensation.

Minimum heat flux

If in a film boiling situation the heat flux, respectively the temperature is reduced, the minimum heat flux is reached, point G, when the rate of vapor formation reaches a point, where a stable vapor film over the heating surface can just yet be sustained. If the heat flux is a bit less than this amount, an unstable situation occurs, and the liquid vapor interface collapses. Rewetting occurs on the heating surface, cooling it and re-establishing nucleate boiling nearly at the same level of the heat flux. This point called Leidenfrost temperature is important for material processing.

4. Experimental Instrumentation

In preparation of a shuttle flight for the MAUS (Get Away Special) program, scheduled first in 1986, we began to study boiling on wires and flat plates with TEXUS 3 in 1980 /4–7/. Even TEXUS flights are not so numerous as to study all parameters and modes of boiling heat transfer, therefore, we strengthened our research program with several campaigns of parabolic aircraft flights KC 135 at the Johnson Space Center in Houston in 1985 /8–11/. During the parabolic trajectory low gravity of about $a/g = \pm 0,03$ over a period of 20 sec can be obtained, followed by a high gravity period with $a/g = 1.8$. Thus in one sequence, a variation from low to high gravity can be researched and a direct comparison between low and high gravity results is possible under the same experimental conditions. During one flight of about 2.5 hours, a series of 30 parabolas are flown. In these parabolic flights, the experimenter handles the hard- and software himself, thus insuring the complete experiment control and optimal scientific results.

For TEXUS and parabolic flights different cells, however, with similar design were used as shown in Fig. 2. The experimental cell was completely filled with liquid and a metal bellows compensated the volume change during boiling and kept the pressure constant according to the counterpressure on the opposite side of the bellows. Thus, by control of the counterpressure with compressed air, the liquid pressure could be changed from saturation to subcooled at a constant liquid bulk temperature.

Fig. 2 Experimental cell for TEXUS. For KC 135, a similar design for higher pressure up to 45 bar was used with a larger volume of 2 ltr. The volume compensation was done in a separate cell by means of a bellows.

While in the TEXUS cell a single heater was used during one flight (wire or plate), three different heaters were simultaneously installed in the KC 135 and studied one after each other (platinum wire with diameter of 0.05 and 0.2 mm and 50 mm lenght, a gold coated flat plate 40 x 20 mm^2 and in some flights a gold coated glass tube with a diameter of 8 mm and 50 mm lenght instead of one wire). The platinum wires and the gold coatings were simultaneously used as resistance heater and resistance thermometer, measuring heat flux levels and average heater temperatures using voltage and current. The bulk liquid state is measured by several thermocouples and pressure transducer. The cell temperature can be controlled up to 110 °C.

Optical recording was possible through glass windows in the pressure cell by a 16 mm Teledyn film camera with 18 and 100 fps in TEXUS, and by a Arriflex camera synchronized with a stroboscope flash in the parabolic flight set-up.

In the TEXUS arrangement, the experiment was controlled by a timer module in the electronics, the data were transmitted to the ground by telemetry. In the aircraft, modified laboratory hardware and standard commercial equipment were used like: power supplies, digital voltmeter, scanner and a personal computer to control the experiment and record the data. The gravity level was determined by a 3-axis accelerometer. Due to the low maximum pressure of 2 bar of the TEXUS cell, R 113 was studied here at a bulk liquid temperature of about 26 °C and a pressure $p/p_c = 0.013$. To cover a wide range of pressures from $p/p_c = 0.11$ to 0.7, the refrigerant R 12 was used as test fluid in the aircraft flights; p/p_c is the reduced pressure, p the saturation pressure and p_c the critical pressure. The bulk temperature and pressure of the liquid were kept constant and at each parabola only one heater was in operation. After completing one boiling curve with 6 to 8 heat flux levels, one of the other heaters was used at the same fluid state. By changing the bulk pressure, we investigated saturated and subcooled conditions at the same bulk temperature. The main interest in this study was to directly compare values of the heat transfer coefficients at low and 1g conditions during one parabola sequence. In the TEXUS flight, 1g data were obtained just before launch and after recovery.

5. Gravity as a parameter in the heat transfer correlations

All correlations for boiling heat transfer are based on physical mechanisms or developed empirically under the conditions of earth gravity; gravity is therefore used as a constant factor and is not considered as a parameter. However, if buoyancy is directly used in the physical models as the driving force for heat transfer, or if the "departure diameter" of the bubbles is introduced in empirical relations, then gravity is raised to a significant physical parameter. A comparison of those relations, extrapolated to lower or higher gravity levels, with experimental data will give a significant indication concerning the interpretation of the physical mechanisms of boiling, and of the correct modelling of the dominating effects. If we assume that gravity is a parameter and that all other parameters are constant, we can analyze the correlation in respect to the effect of gravity, which can be expressed in a power law as:

$$\alpha/\alpha_1 = (a/g)^n \tag{4}$$

where α/α_1 is the ratio of the heat transfer coefficients, with α_1 the value at earth gravity g and a/g is the fraction of the acceleration change. The sign and the value of the exponent n indicates the change of the heat transfer ratio.

The numerous correlation developed for nucleate pool boiling will not be discussed in detail in the framework of this paper. Briefly stated, they can be classified in 3 categories:

1. Physically based equations, the exponent is 0.5 for saturated and 0 for subcooled fluid states.
2. Dimensionless group correlations, n is very arbitrary ranging from –0.35 to +0.5.
3. Empirical relations, evluation of n is senseless.

For the process of nucleate boiling the physically based equations are supported by the following observations: after a bubble is formed in the superheated liquid layer by activation of a nucleate site, the bubble grows by evaporation in the superheated liquid boundary layer. The bubble departs from the surface, when a size is reached, at which the upward forces caused by gravity and buoyancy exceed the adhesive forces. During the departure, a part of the superheated boundary layer follows in the wake as drift flow, transporting the bubble's enthalpy and superheated liquid into the cooler liquid bulk, while cold liquid flows back into the cavity and is heated by transient heat conduction. At lower heat fluxes, when bubbles do not occupy the entire surface, free convection can also contribute to the heat transfer. Normally, under upward heating conditions, the mean upward force is the buoyancy force, and even drift and free convection flow depend on buoyancy. While the theoretical models with $n = 0.5$ indicate a large decrease in the heat transfer coefficient, the dimensionless group correlations shows no uniform behavior.

6. Nucleate boiling

6.1 Results from parabolic flights

Saturated fluid state

A typical parabola sequence of nucleate boiling on a wire of 0.2 mm dia. is shown in Fig. 3 (fluid R 12, saturated state at a reduced pressure $p/p_c = 0.18$). The gravity level a/g, the temperature difference $\Delta T_{sat} = T_w - T_{sat}$ and the power $\dot{q}_w$ of the heater are plotted versus the experimental time. The power was switched on during the low gravity period at 40 sec on the time scale, thus eliminating convection before this stage. Due to the small heat capacity of the wire, the temperature response was very fast after power on and at the change of power at 45 sec. At a constant power level from 45 to 94 sec the temperature remains constant even when the acceleration increases from $a/g \approx 0.01$ to 1.8 and decreases to 1 again. The small wiggles in the temperature curve are due to the last digit in the resolution of the temperature. The photographs show the dependence of bubble size on gravity, large bubbles at low gravity and small bubbles at high gravity. Between $a/g = 1.8$ and 1 the average bubble size is barely reduced. It is clearly demonstrated that the heat transfer coefficient α, according eq.(1) with constant ΔT_{sat} and constant $\dot{q}_w$, is neither influenced by gravity nor by the bubble size at this fluid state. α/α_1 remains nearly unity, but even ratios of $\alpha/\alpha_1 > 1$ have been observed at lower heat flux levels.

Fig. 3 A parabola sequence, a/g level, wire temperature, heat flux at nucleate boiling $p/p_c = 0.18$, versus time

Fig. 4 Saturation boiling with R12 at various reduced pressures p/p_c. The symbols are the data measured at microgravity, the lines represent the values at $1g$ in the consecutive sequence of the parabola

Fig. 5 Heat transfer ratio on the wire dia. 0.2 mm, values from Fig. 4

These investigations are carried out for saturated and subcooled fluid states from $0.1 < p/p_c < 0.7$ and for four heater configurations: wires with 0.05 mm dia. and 0.2 mm dia., flat plate gold coated surface 40 x 20 mm^2 and tube 8 mm dia. and 50 mm length. The results are evaluated for all heaters by Zell (1991, /10/) and plotted as boiling curves with the heat flux density $\dot{q}_w$ versus the temperature difference $\Delta T_{sat} = T_w - T_{sat}$. Only one example will be shown for the wire 0.2 mm dia. with the bulk liquid being at saturated state for different p/p_c values in Fig. 4. The symbols represent the data obtained at low gravity $a/g = \pm 0.02$, while the lines represent $a/g = 1$ reference data measured immediately after low gravity in the consecutive period of the parabola. The evaluation with respect to the heat transfer ratio α/α_1 versus heat flux density is shown for this heater in Fig. 5. From this figure, it can be seen that the heat transfer coefficient for wires is even higher than at earth gravity for low heat flux levels. This may be attributed to the fact that at low gravity all nuclei sites around the wire are equally activated. As a result, boiling occurs symmetrically around the wire at low gravity, whereas at 1g the lower stagnation point is cooled by free convection and only the upper circumference of the wire is preferred for boiling. Similar behavior can be observed with the other geometries: if convection is eliminated, more nuclei sites are activated at low heat fluxes. The reduction of the heat transfer coefficient at higher heat flux is caused by the larger bubbles and the connected increase of dry areas at the heater below them. At higher system pressure, especially observed on the wires at $p/p_c = 0.68$, α/α_1 decreases by 25% with higher heat flux. This may be due to the small surface tension closer to the critical point. We have observed similar behavior on other geometries for subcooled fluid states. According to the present theory and eq.(4), the heat transfer ratio should be reduced to $\alpha/\alpha_1 = 0.1$ at an acceleration level of $a/g = 10^{-2}$, see Fig. 5. However, the heat transfer coefficient is nearly independent from gravity even in saturated and subcooled nucleate boiling.

6.2 Results from TEXUS flights

6.2.1 Nucleate boiling on wires

In the TEXUS flights we have used R 113 as a test fluid with bulk temperature about $T_B = T_{sat} = 26$ °C with heat fluxes from 40 to 276 kW/m^2. At low heat fluxes on wires, the heat transfer coefficient is the same as in the reference experiment at 1g and is about 96% at higher heat fluxes. Due to the good quality of the acceleration level $a/g < 10^{-4}$ the heat transfer coefficient should be strongly reduced to $\alpha/\alpha_1 = 0.01$ according to the theory, eq.(4).

By increasing the pressure to $p = 1$ bar at 26 °C bulk temperature, a subcooling of $\Delta T = 22$ K was established. Between 40 and 441 kW/m^2 steady state nucleate boiling was achieved. At the next step of the heat flux of 450 kW/m^2 film boiling occured, and the power was switched off by an automatic control system. The heat transfer coefficient is the same at lower heat fluxes and only 2 % less at higher heat fluxes compared to $1g$. We observed the development of a strong Marangoni convection for subcooled liquid states.

6.2.2 Boiling on a flat plate at low pressures

Compared to saturated boiling on a wire, the boiling phenomena on a flat plate at very low system pressure of $p/p_c = 0.013$ in R 113 is different. After onset of boiling at a heat flux of 28 kW/m^2, the first bubble grows slowly to almost the entire size of the heater. In the film, one can observe that small bubbles are formed in the liquid triangle between the heater and vapor, and immediately coalesce with larger bubbles.

The heat flux is increased in steps of 10 kW/m^2 every 20 seconds. In the μg experiment, the temperature increases after each heat flux step, however, with a decreasing gradient, which indicats a tendency to an asymptotic constant value. It can not be excluded that with a larger heater surface and a longer period of constant heat flux, steady state boiling would have been achieved, however, with heat transfer coefficients much less than at earth conditions in the order of $\alpha/\alpha_1 \approx 0.5$, but not as low as predicted by theory $\alpha/\alpha_1 = 0.01$.

At the 60 kW/m^2 heat flux step the system runs into a burn-out situation with a strong increase of surface temperature and an increasing gradient. An automatic control system switches power off. By reducing the power to 50, 30 and 20 kW/m^2, the surface temperature decreases and it appears that a constant surface temperature can be achieved.

By the very large bubbles (30 to 40 mm in diameter) at the low system pressure, a large portion of the heater surface is covered by vapor and this dry area raises the average temperature of the heater.

Some experiments of subcooled boiling are performed with subcoolings of 17 K and 48 K by variing the pressure.

A bubble of semi-spherical shape covered the heater in less than 0.1 seconds. Bubbles formed at the edge of the bubble, are lifted by the growing bubble looking pock-marked. After 1.2 sec the bubble grows large at the base, the smaller bubbles at the base coalesce, or more precisely, feed the larger one. At the top, the bubbles condensate in a very dynamic process. Steady state conditions are reached after about 4 sec. In the series of photographs in Fig. 6 the development to steady state boiling after onset of boiling is seen.

Fig. 6 Development of subcooled boiling, time after onset of boiling, at 4.2 sec steady state boiling is reached

Very few bubbles depart from the surface, sometimes they are lifted up and replaced by smaller bubbles growing below. At the same time always one or two larger bubbles can be observed, establishing a mass flow through the bubble by coalescence at the base and

condensation of vapor at the crown. At 50 kW/m^2 the heater temperature increases, however, with a decreasing gradient. A stationary heater temperature might have been achieved, if the period for one heat flux step could be prolonged. The low gravity curves, in comparison to $1g$, are characterized by higher temperatures and lower heat transfer coefficients, however, much higher compared to theory.

7. The micro-wedge model

The existing theoretical and empirical correlations valid for nucleate boiling are only developed under earth gravity conditions, and therefore claim validity only for $a/g = 1$. If we suppose that the physics of the boiling process is properly described, an extrapolation to lower accelerations should implicitly be possible without too large deviations from the experimental findings. However, the comparison with microgravity experiments result in great differences and support the statement given in the introduction that the physics of nucleate boiling is not properly understood yet, and not well represented in the correlations known today. If gravity and buoyancy are not as significant as assumed, the question arises, what the real physical mechanisms for the boiling process are.

The primary mechanisms are the formation and growth of bubbles in the superheated liquid boundary layer by evaporation at the liquid vapor interface. Most important for the heat transfer is the small wedge between the solid-liquid, solid-vapor and liquid-vapor interfaces, we call now „micro-wedge", see Fig. 7 In this region the heat transfer rate determined by the evaporation rate is very high and independent from gravity. It is influenced by the heater temperature, the heat transport through the thin liquid film in the wedge between the heater and the bubble interface, the evaporation at the interface and the liquid flow to the interface due to capillary forces.

Fig. 7 Micro-wedge modell of nucleate boiling. Nucleate boiling is stable for $\dot{m}_v = \dot{m}_r$ and unstable for $\dot{m}_v > \dot{m}_r$ (CHF, transition to film boiling)

In a simplified manner, we can treat this model similar to a evaporating liquid film /12, 13/. In this thin film, pure heat conduction is assumed, thus the heat flux density $\dot{q}$ in the z-direction can be written as:

$$\dot{q}(r) = \frac{\lambda}{\delta(r)} (T_w - T_p) \tag{5}$$

where λ is the thermal conductivity of the liquid and $\delta(r)$ the thickness of the liquid film. T_w is the surface temperature of the heater, which is even a function of r, and T_p is the temperature on the liquid side at the interface, which is depending on $\delta(r)$ and the evaporation rate. In a first approach, we assume $T_p \approx T_{sat}$, the saturation temperature corresponding to the system pressure.

The evaporation rate $\dot{m}_B$ for a single bubble is expressed by the kinetic theory of evaporation as:

$$\dot{m}_B = \int_{(B)} 2\pi r \cdot \dot{m}_v \, dr = \int_{(B)} 2\pi r \cdot \beta_v \sqrt{\frac{k}{2\pi m^*}} \left(\frac{p_p}{\sqrt{T_p}} - \frac{p_v}{\sqrt{T_v}} \right) dr \tag{6}$$

where β_v is the evaporation coefficient, k the Boltzmann constant and m^* the mass of the molecule. p stands for the pressure and T for the temperature, both having indices p for the interface of the liquid and v for the vapor side. Using eq.(6), the heat flux rate per bubble is expressed with the evaporation enthalpy Δh as:

$$\dot{Q}_B = \dot{m}_B \cdot \Delta h \tag{7}$$

The flow in direction towards the interface is caused by capillary forces due to non-equilibrium conditions at the interface, which result from the strong evaporation and a deviation of curvature from the equilibrium value. With the assumption that the flow in the wedge is in steady state, slow and parallel to the wall, the momentum equation is simplified to :

$$\frac{\partial p_f}{\partial r} = -\eta \frac{\partial^2 u_r}{\partial r^2} \tag{8}$$

with η as the dynamic viscosity, u_r the velocity in r-direction and p_f the pressure of the liquid. $\partial p_f / \partial r$ is due to the change of capillary pressure according to the change of curvature. With eq.(5) – (8), the handling of the micro-wedge model is only indicated. In reality, an unsteady flow and bubble growth have to be considered addionally. During the first rapid growth of a bubble the liquid flow is not developed, moreover the liquid is pushed aside by the expansion of the bubble. However, in case of larger bubbles under microgravity the flow in the wedge is evident and can be observed via the migration of smaller bubbles. The numerical integration of the differential equations yield to the heat transport of one bubble and when multiplied by the active nucleation sites should result in the overall heat transfer. In subcooled liquids, additional heat transport mechanisms are the thermocapillary flow from the base to the cap of the bubble and the heat pipe effect by evaporation and condensation inside the bubble. At a certain high heat flux, so called critical heat flux, the thin liquid film can completely evaporate, meaning that the evaporating mass flow is higher than the liquid mass flow towards the interface resulting in a dry area below the bubble. This unstable situation is rapidly spreading over the entire heater surface and a closed vapor film is formed. As a consequence, the temperature of the heater is rapidly increasing and the nucleate boiling regime changes to the film boiling mode.

8. Secondary mechanisms

Secondary mechanisms are responsible for the heat and mass transport form the heater surface to the bulk liquid by departing bubbles carrying away latent heat, by wake flow following the bubbles and by convection. In pool boiling under earth gravity, the buoyancy is the driving force for this processes. In microgravity various effects are observed mainly caused by surface tension, like vertical and horizontal bubble coalescence and displacement of larger bubbles by smaller ones. If bubbles coalesce, liquid is set into motion and by its inertia and momentum the bubbles are lifted from the surface. More details about these effects are described in recent publications /14/.

planned to study the thickness of the liquid film and simultaneously the temperature field around the bubble by interferometry.

Acknowledgments

This project and the Japanese German Coorperation have been sponsored by the Bundesminister für Forschung und Technologie, BMFT, represented by DLR/DARA. The experiment module for TEXUS was designed by MBB ERNO, Bremen. The parabolic flights were supported by ESA and DLR. We also gratefully thank all teams involved in the project for their kind assistance.

References

/1/ Nukiyama, S. (1934):
The Maximum Values of the Heat Q Transmitted from Metall to Boiling Water Under Atmosheric Pressure; Trans. JSME, Vol. 37, p. 367, reprinted in Int. J. Heat Mass Transfer, Vol. 9, pp 1419–1433

/2/ Dhir, V.K. (1990):
Nucleate and Transition Boiling Heat Transfer Under Pool Boiling and External Flow Conditions; Proc. 9th Int. Heat Transfer Conf., Jerusalem 1990, Hemisphere Pub., New York

/3/ Fritz, W. (1935):
Berechnungen des Maximalvolumens von Dampfblasen; Phys. Z. 36, pp. 379 – 384

/4/ Weinzierl, A.; Straub, J.; Zell, M. (1986):
Spacelab Nutzung: Untersuchung des Wärmeübergangs und seiner Transportmechanismen bei Siedevorgängen unter Schwerelosigkeit; BMFT-Forschungsbericht W86-021

/5/ Weinzierl, A.; Straub, J. (1982):
Subcooled Pool Boiling in Micro-Gravity Environment; Proc. 7th Int. Heat Transfer Conference, Munich (1982), Vol.4, pp. 21–27

/6/ Weinzierl, A. (1984):
Untersuchung des Wärmeübergangs und seiner Transportmechanismen bei Siedevorgängen unter Schwerelosigkeit; Dissertation TU München

/7/ Zell, M.; Weinzierl, A.; Straub, J. (1984):
Nucleate Pool Boiling in Subcooled Liquid under Microgravity – Results of TEXUS Experimental Investigations; Proc. 5th European Symposium on Material Sciences under Microgravity – Schloß Elmau, (1984), ESA SP–222, pp. 327–333

/8/ Zell, M.; Straub, J.; Vogel, B. (1989):
Pool Boiling Under Microgravity; J. PhysicoChemical Hydrodynamics, Vol. 11, No. 5/6, pp 813–823

/9/ Straub, J.; Zell, M. and Vogel, B. (1990):
Pool Boiling in a Reduced Gravity Field; Proc. 9th Int. Heat Transfer Conf., Jerusalem 1990

/10/ Zell, M. (1991):
Untersuchung des Siedevorgangs unter reduzierter Schwerkraft; Ph.D. thesis, Technische Universität München

/11/ Straub, J; Zell, M. and Vogel, B. (1992):
Boiling under Microgravity Conditions; Proc. 1st Europ. Symp. Fluids in Space, Ajaccio, France, Nov. 18-22, 1991, ESA SP-353, S. 269-297

/12/ Wayner, P.C. (1979):
Effect of Interfacial Phenomena in the Interline Region on the Rewetting of a Hot Spot; Int. J. Heat Mass Transfer, 22, S. 1033-1040

/13/ Stephan, P. (1992):
Wärmedurchgang bei Verdampfung aus Kapillarrillen in Wärmerohren; Fortschrittsberichte VDI Reihe 19, Wärmetechnik 59

/14/ Straub, J. (1993):
The Role of Surface Tension for Two-Phase Heat and Mass Transfer in the Absence of Gravity; Invited paper presented at the 3rd World Conf. on Experimental Heat Transfer, Fluid Mechanics and Thermodynamics, Nov. 1993, Honolulu, Hawaii, USA, to be published in the proceedings

/15/ Oka, T.; Abe, Y.; Tanaka, K.; Mori, Y.H. and Nagashima, A. (~~1993~~ 1992):
Observational Study of Pool Boiling under Microgravity; JSME Int. Journal, Series 2, Vol. 35, No. 2, pp 280-286

/16/ Oka, T. (~~1992~~ 1993):
Heat Tranport in Pool Boiling under Microgravity; Ph.D. thesis, Keio University, Japan (in Japanese)

/17/ Oka, T.; Abe, Y.; Iwashita, K.; Mori, Y.H. and Nagashima, A. (1993):
Pool Boiling Heat Transfer of Nonazeotropic Binary Mixtures in Microgravity; 30th National Heat Transfer Symp., Vol 3, pp 835-837 (in Japanese)

Fig. 1 Sketch of a boiling curve with the various modes of heat transfer

Fig. 2 Experimental cell for TEXUS. For KC 135, a similar design for higher pressure up to 45 bar was used with a larger volume of 2 ltr. The volume compensation was done in a separate cell by means of a bellows.

Fig. 3 A parabola sequence, a/g level, wire temperature $\Delta T = T_w - T_{sat}$, heat flux $\dot{q}$ at nucleate boiling $p/p_c = 0.18$, versus time

Saturated

Fig. 4 Saturation boiling with R12 at various reduced pressures p/p_c. The symbols are the data measured at microgravity, the lines represent the values at $1g$ in the consecutive sequence of the parabola

Fig. 5 Heat transfer ratio on the wire dia. 0.2 mm, values from Fig. 4

$\Delta T_{Sub} = 48K$

Fig. 6 Development of subcooled boiling, time after onset of boiling, at 4.2 sec steady state boiling is reached. In the lower row steady state boiling at 30, 50, 60, 70 kW/m^2.

Fig. 7 Micro-wedge modell of nucleate boiling. Nucleate boiling is stable for $\dot{m}_v = \dot{m}_r$ and unstable for $\dot{m}_v > \dot{m}_r$ (CHF, transition to film boiling)

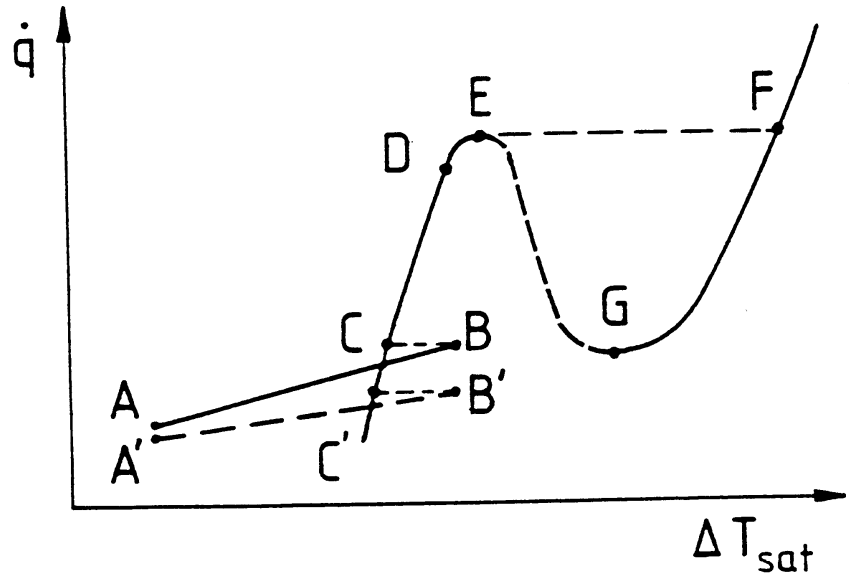

A-B	free convection ($1g$)
A′-B′	conduction (μg)
B, B′	onset of boiling
C-D	nucleate boiling
D-E	increasing instability
E	critical heat flux, CHF
F-G	film boiling
G	minimum heat flux, begin of rewetting
G-E	transition boiling

~~Fig. 1 Sketch of a boiling curve with the various modes of heat transfer~~

Straub, J. : Fig. 1

Fig 1

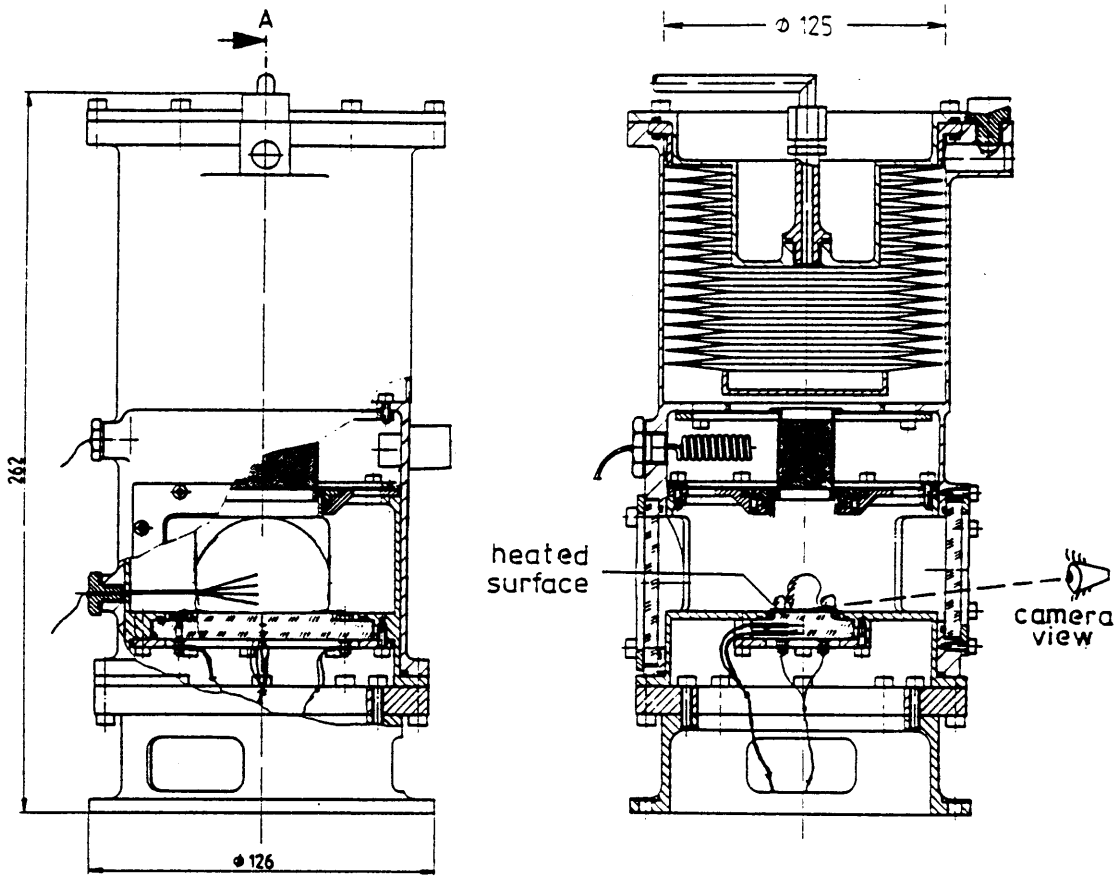

Fig. 2 Experimental cell for TEXUS. For KC 135, a similar design for higher pressure up to 45 bar was used with a larger volume of 2 ltr. The volume compensation was done in a separate cell by a bellows.

Fig. 2

Straub, J. : Fig 2

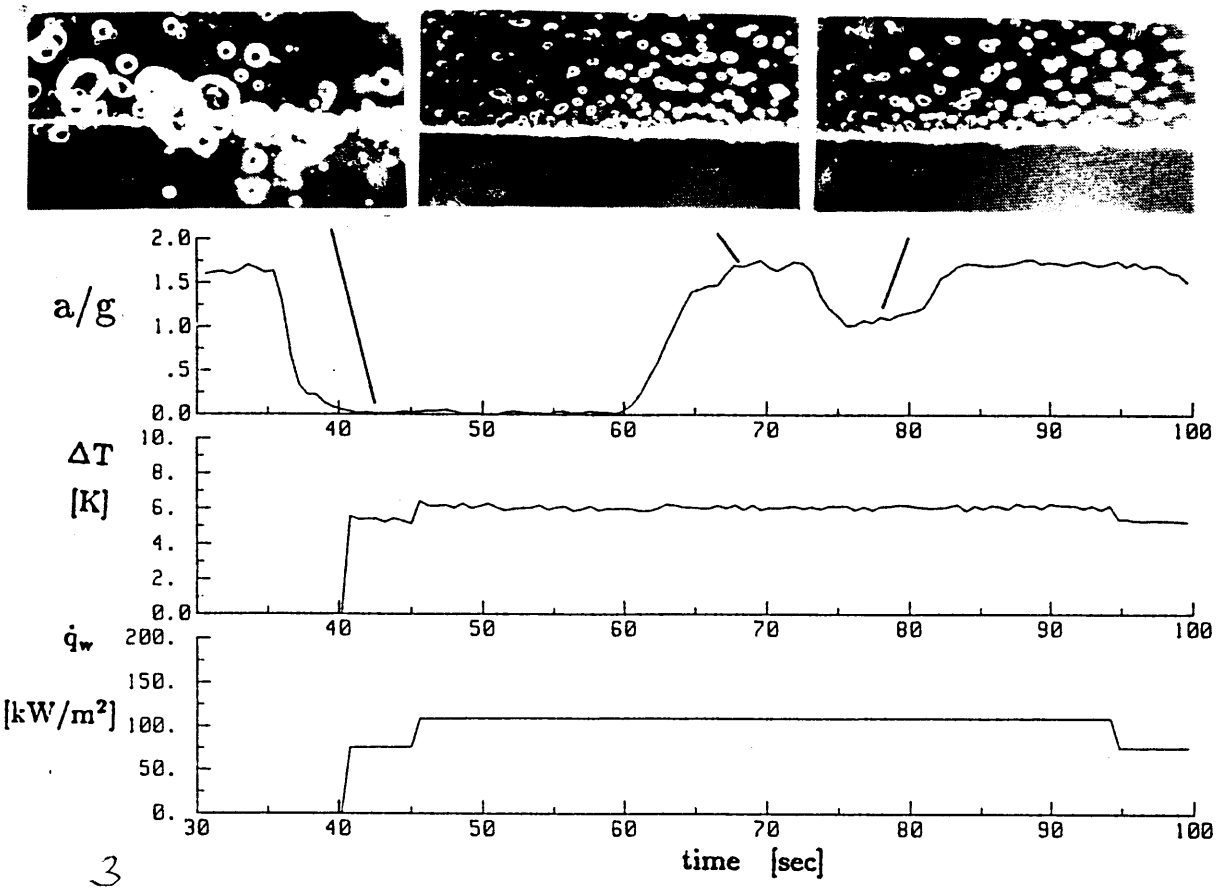

Fig. 3 A parabola sequence, a/g level, wire super heat temperature $\Delta T = T_w - T_{sat}$, heat flux at nucleate boiling $p/p_c = 0.18$, versus time

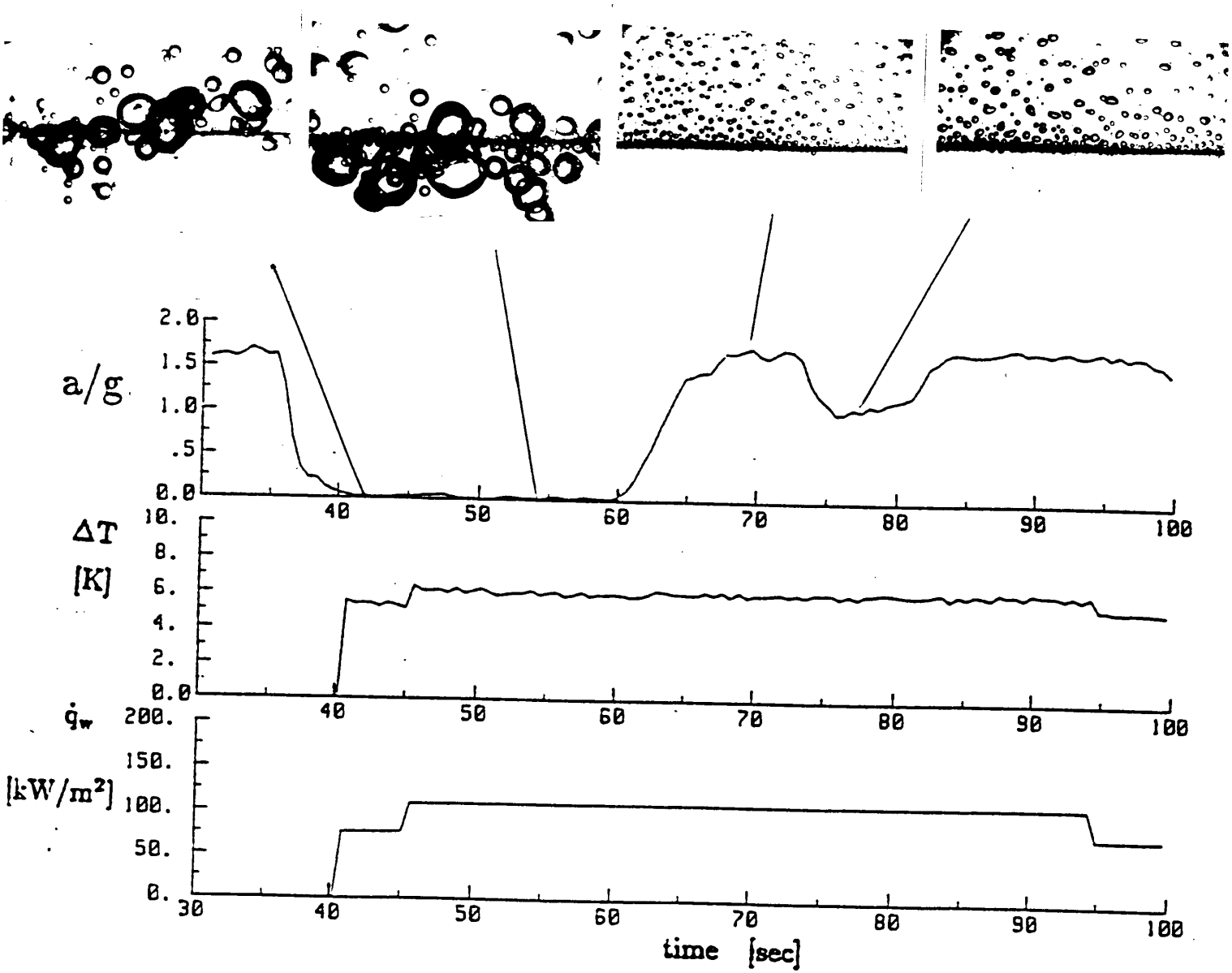

3

Fig. 2 A parabola sequence, a/g level, wire super heat temperature $\Delta T = T_w - T_{sat}$, q^* heat flux at nucleate boiling $p/p_c = 0.18$, versus time

saturated

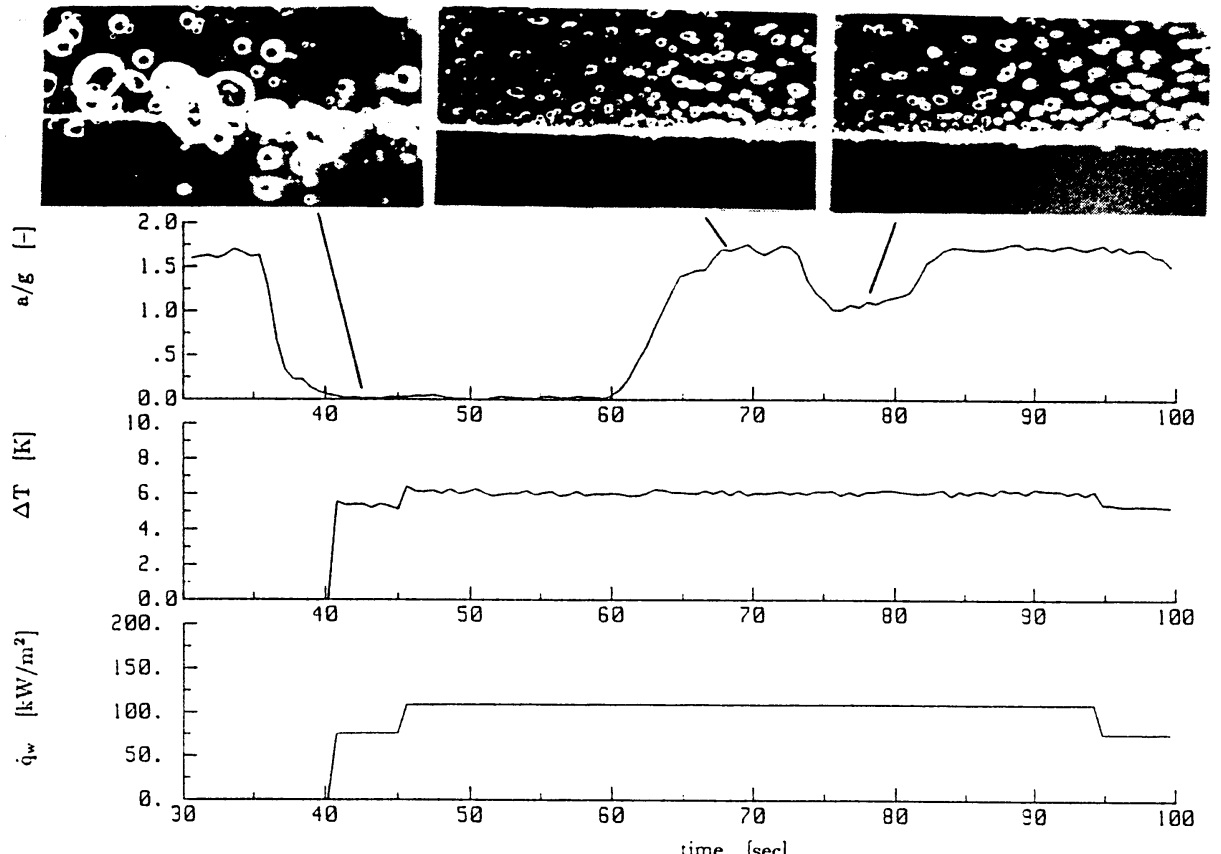

Fig. 5 A parabola sequence, a/g level, wire temperature, heat flux at nucleate boiling $p/p_c = 0.18$, versus time.

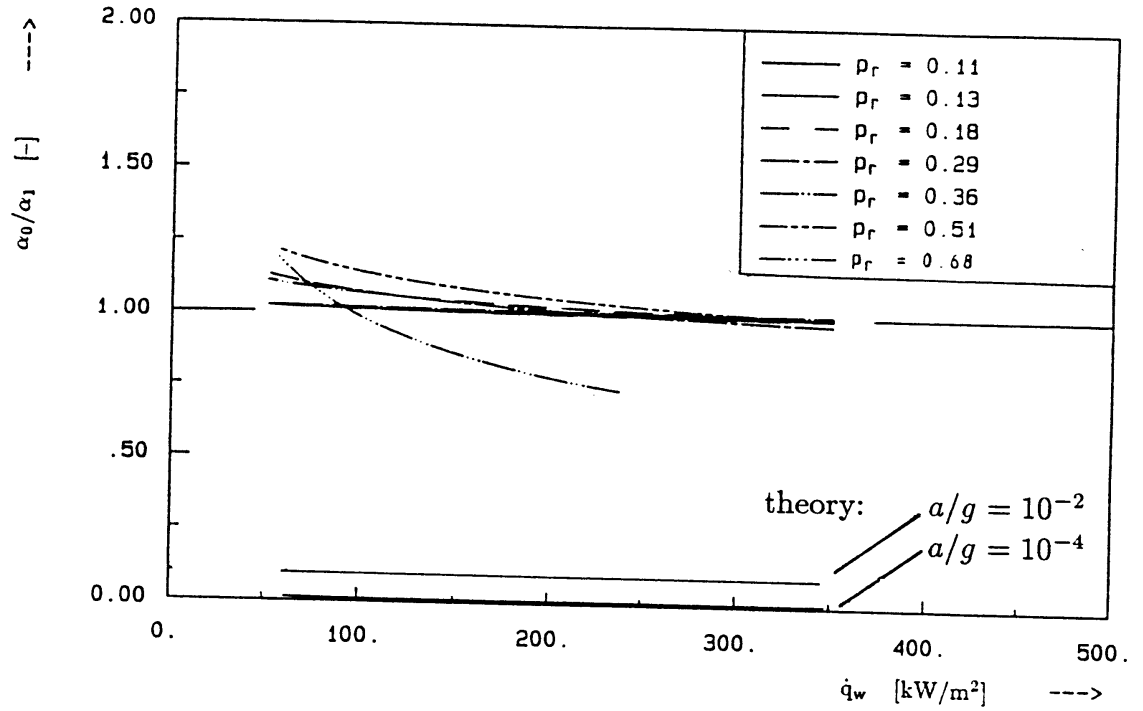

~~Fig. 8 Heat transfer ratio on the wire dia. 0.2 mm, values from fig. 6~~

Staub, J. : Fig. 5

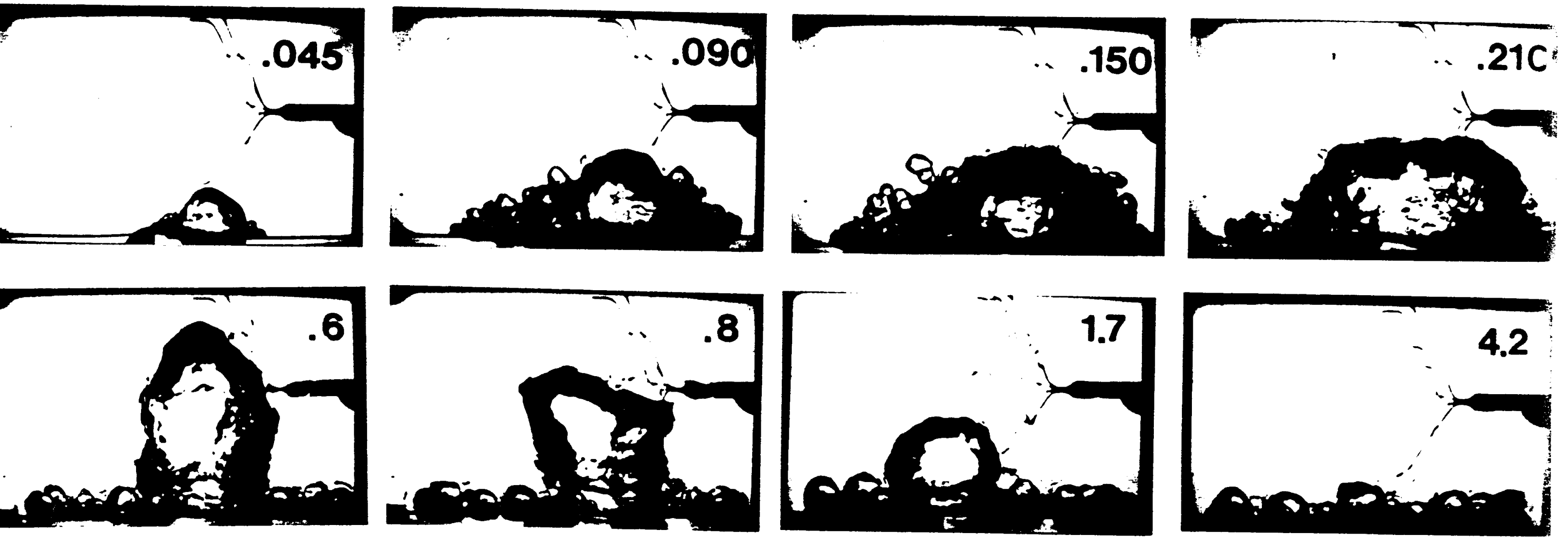

Straub, J.: Fig 6

Fig 6 Development of [illegible] time after onset of boiling, at [illegible] sec steady state boiling [illegible]

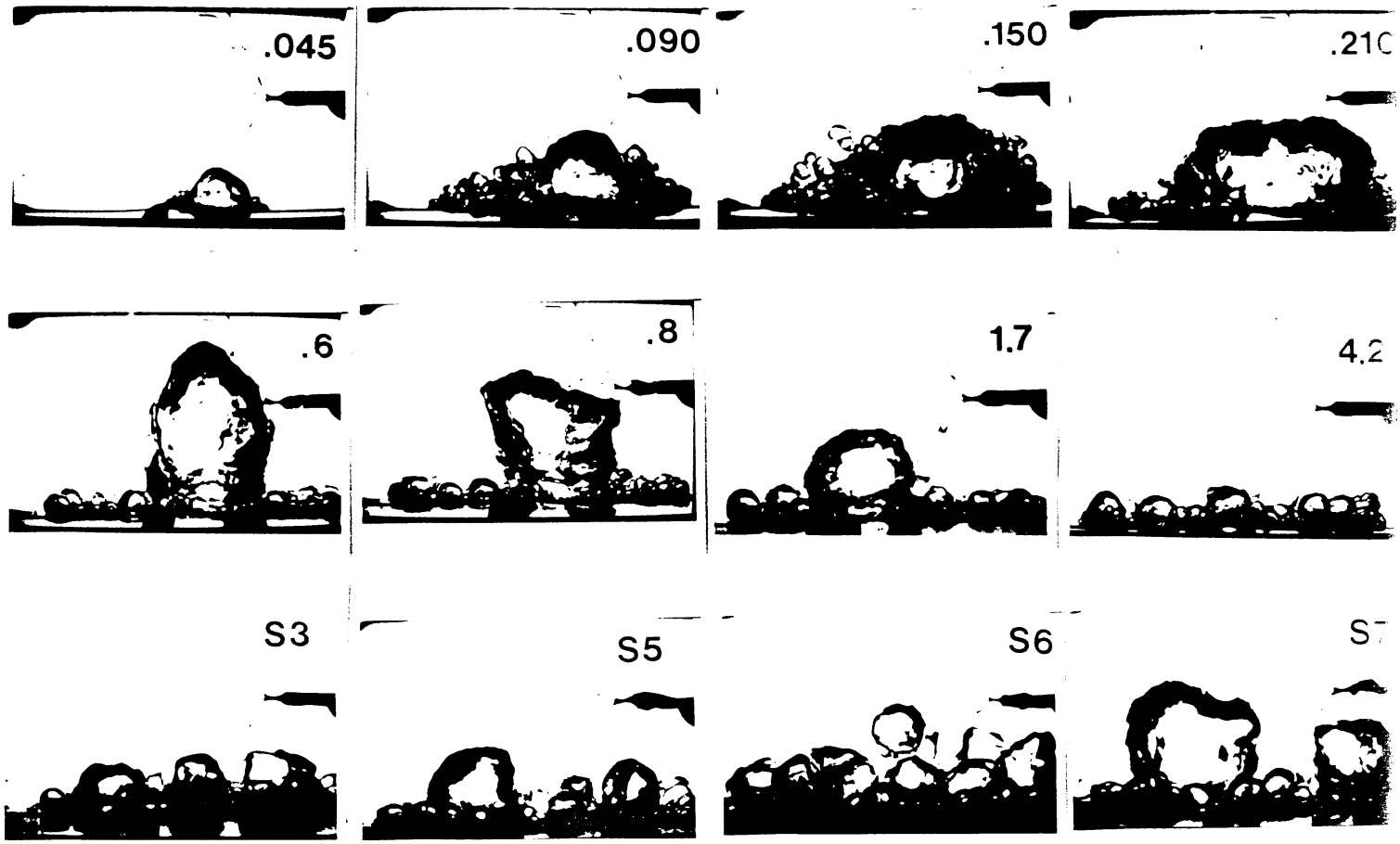

$\Delta T_{sub} = 48K$

Fig 6 Development of subcooled boiling, time after onset of boiling, at 4,2 steady state boiling is reached, In the lower row steady state boiling at 30, 50, 60, 70 kW/m²

Straub J.

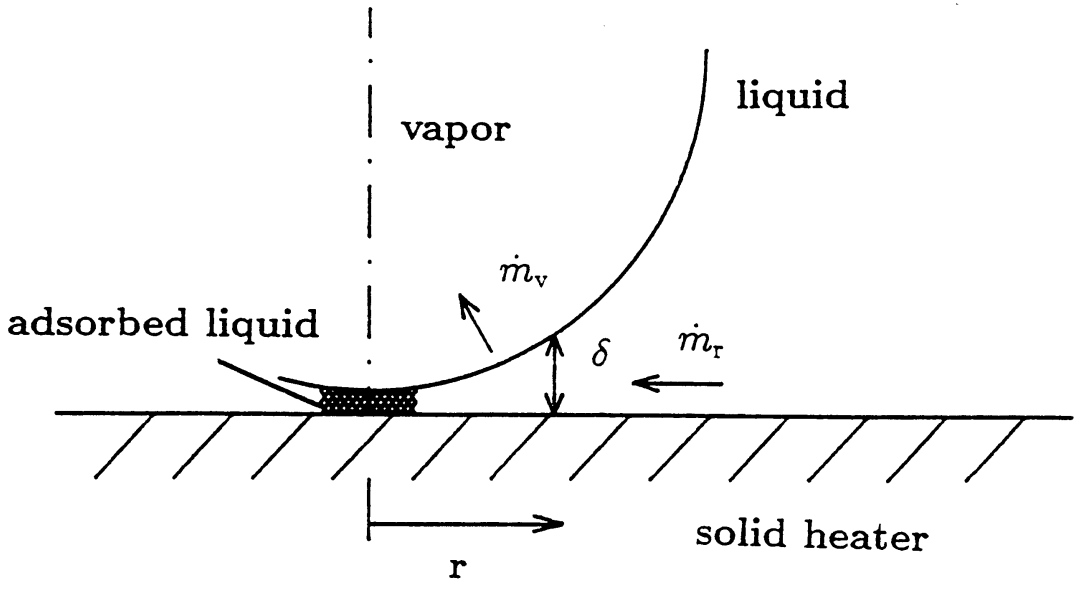

Straub, J. : Fig. 7

Fig 7 Micro-wedge modell of nucleate boiling.
Nucleate boiling is stable : $\dot{m}_v = \dot{m}_r$
unstable $\dot{m}_v > \dot{m}_r$ transition to CHF.